



Published in final edited form as:

Science. 2010 October 1; 330(6000): 55–60. doi:10.1126/science.1193270.

Piezo1 and Piezo2 are essential components of distinct mechanically-activated cation channels

Bertrand Coste¹, Jayanti Mathur², Manuela Schmidt¹, Taryn J. Earley¹, Sanjeev Ranade¹, Matt J. Petrus², Adrienne E. Dubin¹, and Ardem Patapoutian^{1,2,3}

¹Department of Cell Biology, The Scripps Research Institute, La Jolla, CA 92037

²Genomics Institute of the Novartis Research Foundation, San Diego, CA 92121

Abstract

Mechanical stimuli drive many physiological processes, including touch and pain sensation, hearing, and blood pressure regulation. Mechanically-activated (MA) cation channel activities have been recorded in many cells, but the responsible molecules have not been identified. We characterized a rapidly-adapting MA current in a mouse neuroblastoma cell line. Expression profiling and RNAi knockdown of candidate genes identified *Piezo1* (*Fam38A*) to be required for MA currents in these cells. Piezo1 and related Piezo2 (*Fam38B*) are vertebrate multipass transmembrane proteins with homologs in invertebrates, plants, and protozoa. Overexpression of mouse Piezo1 or Piezo2 induced two kinetically-distinct MA currents. Piezos are expressed in several tissues, and knockdown of Piezo2 in dorsal root ganglia neurons specifically reduced rapidly-adapting MA currents. We propose that Piezos are components of mechanically-activated cation channels.

Introduction

Mechanotransduction, the conversion of mechanical force into biological signals, has crucial roles in physiology. In mammals, embryonic development, touch, pain, proprioception, hearing, adjustment of vascular tone and blood flow, flow sensing in kidney, lung growth and injury, bone and muscle homeostasis as well as metastasis are all regulated by mechanotransduction (1-2). In plants, mechanical force strongly impacts morphogenesis, for example in lateral root formation (3). Unicellular organisms such as ciliates sense touch and change direction in response to a tactile stimulus (4). Mechanotransduction in vertebrate inner ear hair cells is extremely rapid, implicating an ion channel directly activated by force (5). Indeed, calcium-permeable mechanically-activated (MA) cationic currents have been described in various mechanosensitive cells (2-3,6-7). However, only few MA channels have been identified to date (for review, see (1-2)), and definitive candidates in vertebrate mechanosensation has yet to emerge.

Neuro2A cells express MA currents

To identify proteins involved in mechanotransduction, we sought a cell line that expresses a MA current similar to those recorded from primary cells (8). We screened several mouse and rat cell lines (Neuro2A, C2C12, NIH/3T3, Min-6, 50B11, F11, PC12) applying force to the cell surface via a piezo-electrically driven glass probe while patch-clamp recording in

³To whom correspondence should be addressed, ardem@scripps.edu .

Supporting Online Material www.sciencemag.org Materials and Methods Figs. S1, S2, S3, S4, S5, S6, S7, S8 Table S1, S2

the whole-cell configuration with another pipette (6,8-9). The Neuro2A (N2A) mouse neuroblastoma cell line expressed the most consistent MA currents, and showed relatively faster kinetics of adaptation (decreased activity in response to a sustained stimulus) compared to other cell lines such as C2C12s (Fig. 1A-B and Fig. S1A-D). Current-voltage relationships of N2A and C2C12 MA currents were linear between -80 and $+80$ mV with reversal potentials (E_{rev}) at $+6.6$ and $+6.7$ mV, respectively, and inward currents were suppressed with N-methyl-D-glucamine (NMDG)-chloride external solutions, suggesting cationic non-selective permeability (Fig. S1E). We further characterized MA currents in N2A cells in response to suction of the membrane applied through the recording pipette in cell-attached mode (10). Negative pressure pulses evoked opening of endogenous channels (Fig. 1C), with a single-channel conductance of 22.9 ± 1.4 pS and E_{rev} of $+6.2$ mV (Fig. 1D). Increasing the magnitude of pressure pulses induced larger and reversible currents (Fig. 1E). The current-pressure relationship is characterized by maximal opening at -60 mm Hg, with a pressure for half-maximal activation (P_{50}) of -28.0 ± 1.8 mm Hg (Fig. 1F). These conductance and P_{50} values are similar to the properties of reported stretch-activated channels (11-13).

Piezo1 (Fam38A) is required for MA currents of N2A cells

To generate a list of candidate MA ion channels in N2A, we searched for transcripts that are enriched in N2A cells using Affymetrix microarrays. We selected proteins predicted to span the membrane at least two times (a characteristic shared by all ion channels). We prioritized this list by picking either known cation channels, or proteins with unknown function. We tested each candidate (see Table S1) using siRNA knockdown in N2A cells, measuring MA currents during piezo-driven pressure stimulation in the whole cell mode. Knockdown of Fam38A (Family with sequence similarity 38) caused a pronounced decrease of MA currents (Fig. 2A). Attenuation of MA currents was observed with multiple siRNAs directed against this gene (Fig. 2B). All the siRNAs tested decreased the abundance of the target transcripts as assayed by qPCR (Fig. S2A). Given that Fam38A encodes a protein required for the expression of ion channels activated by pressure, we named this gene Piezo1, from the Greek “πίεση” (píesi) meaning pressure. To test whether depletion of Piezo1 impairs general cell signaling or viability, we transfected N2A cells with TRPV1 cDNA (a capsaicin-activated cation channel) and either scrambled or Piezo1 siRNA and observed no differences in capsaicin responses (Fig. S2B-C). We tested whether Piezo1 was also required for N2A MA currents elicited by patch membrane stretch (Fig. 2C). MA currents were diminished in cells treated with siRNA against Piezo1 (Fig. 2D).

Very little is known about mammalian Piezo1 (KIAA0233, Fam38A, Mib). Its expression is induced in senile plaque-associated astrocytes (14), and the protein has been suggested to be involved in integrin activation (15). Extracellular perfusion of cells with buffer lacking divalent ions and containing 5 mM EGTA for 30-60 min, which disrupts integrin function (16), did not suppress MA currents (Fig. S2D-E). Thus it is unlikely that Piezo1 siRNA blocks MA currents through integrin modulation. However, it is possible that mechanical activation of Piezo1 could lead to integrin activation.

Piezos are large transmembrane proteins conserved among various species

Many animal, plant, and other eukaryotic species contain a single Piezo (Fig. 3A). Vertebrates have two members, Piezo1 (Fam38A) and Piezo2 (Fam38B). However, the early chordate *Ciona* has a single member. Multiple Piezos are also present in the Ciliophora kingdom: *Tetrahymena thermophila* has three members; *Paramecium Tetraurelia*, six. No clear homologs were identified in yeast or bacteria. The secondary structure and overall

length of Piezo proteins are moderately conserved, and similarity to other proteins is minimal. As assayed by the Transmembrane Hidden Markov Model prediction program (TMHMM2), all have between 24 and 36 predicted transmembrane domains (with variability perhaps due to inaccurate cDNA or transmembrane prediction). The predicted proteins contain 2100 to 4700 amino acids, and the transmembrane domains are located throughout the putative protein (Fig. S3). Piezo1 expression was observed in bladder, colon, kidney, lung and skin (Fig. 3B). This pattern agrees with northern blot expression analysis in rat (14). Bladder, colon, and lung undergo mechanotransduction related to visceral pain (17), and primary cilia in the kidney sense urinary flux (18). The relatively low amount of mRNA in DRG suggests that Piezo1 may not account for MA currents observed there (8-9,19-22), but Piezo1 was observed in the skin, another putative site of somatosensation. Piezo2 expression was observed in bladder, colon and lung as well, but less abundant in kidney or skin. Strong expression of Piezo2 was observed in DRG sensory neurons, suggesting a potential role in somatosensory mechanotransduction.

Piezo1 induces MA currents in various cell types

We cloned full-length *Piezo1* from N2A cells into the pIRES2-EGFP vector. We recorded MA currents from green fluorescent protein (GFP)-positive cells in the whole-cell mode 12-48 hours after transfection. *Piezo1* but not mock-transfected cells showed large MA currents in N2A, human embryonic kidney (HEK293T) (Fig. 4A-F) and C2C12 cell-lines (Fig. S4A-C). In all cells overexpressing Piezo1, the MA current-voltage relationships were similar to those for endogenous N2A MA currents (Fig. 4B and E, S4B and 1B), with $E_{rev} \sim +6$ mV. The threshold of activation and the time constant for inactivation of MA currents elicited in Piezo1-overexpressing cells was similar in all three cell lines tested (see Table S2). We characterized the ionic selectivity of MA currents in cells overexpressing Piezo1. Substituting the non-permeant cation NMDG in the extracellular bathing solution suppressed inward MA currents, demonstrating that this channel conducts cations (Fig. S4D-E). We further examined ionic selectivity by recording with CsCl-only internal solutions and various cations in the bath. Na^+ , K^+ , Ca^{2+} and Mg^{2+} all permeated, with a slight preference for Ca^{2+} (Fig. S4F-H). Moreover, 30 μ M of ruthenium red and gadolinium, known blockers of many cationic MA currents (9, 23), blocked 74.6 ± 2.5 % ($n = 6$) and 84.3 ± 3.8 % ($n = 5$) of Piezo1-induced MA current, respectively (Fig. S4I-K).

We used membrane stretch through the patch pipette in cell-attached mode to assay Piezo1-transfected cells (Fig. 4G-L). Overexpression of Piezo1 in N2A and HEK293T cells gave rise to large currents elicited by -60 mm Hg pressure pulses (Fig. 4G and J). The current-pressure relationships in cells overexpressing Piezo1 and in endogenous N2A cells were similar, with P_{50} of -28.1 ± 2.8 and -31.2 ± 3.5 mm Hg in N2A- and HEK293T-overexpressing cells, respectively (Fig. 4H and K and 1F). No channel activity similar to N2A endogenous MA channels was detected in HEK293T cells transfected with vector alone.

MA currents in cells overexpressing Piezo2

We cloned full-length *Piezo2* from DRG neurons. N2A and HEK293T cells transfected with Piezo2 and gene encoding GFP showed large MA currents (Fig. 5A-F). The N2A cells were also co-transfected with Piezo1 siRNA to suppress endogenous MA currents. The MA current-voltage relationship in Piezo2-expressing cells was linear between -80 and $+80$ mV (Fig. 5B, E), with a reversal potential (E_{rev}) of $+6.3 \pm 0.4$ mV ($n = 3$) and $+8.7 \pm 1.5$ mV ($n = 7$) in N2A and HEK293T cells, respectively. Piezo2-dependent currents were suppressed by NMDG (Fig. S5A-B), suggesting non-selective cationic conductance. Piezo2-dependent

currents were inhibited by gadolinium and ruthenium red [$85.0 \pm 3.7\%$ ($n = 5$) and $79.2 \pm 4.2\%$ ($n = 5$), respectively] (Fig. S5C-D).

The inactivation kinetics of heterologously-expressed Piezo2-induced MA currents were best fitted with a mono-exponential equation. The calculated time constants for inactivation (τ_{inac}) are relatively fast in both N2A (6.8 ± 0.7 ms, $n = 27$) and HEK293T (7.3 ± 0.7 , $n = 11$) cells when measured at -80 mV. Furthermore, the kinetics of inactivation of Piezo2-dependent MA currents were faster than Piezo1-dependent MA currents, both for inward (Fig. 5G) and outward (Fig. 5H) currents, and at all holding potentials tested (Fig. 5I). Therefore, Piezo1 and Piezo2 confer distinct channel properties.

Piezo1 is detected at the plasma membrane

The results above suggest that Piezo1 and 2 are components of mechanotransduction complexes and therefore should be present at the plasma membrane. Previous reports have shown expression of Fam38A (Piezo1) in the endoplasmic reticulum (14-15). We generated a peptide antibody against mouse Piezo1. This antibody specifically recognized Piezo1-transfected HEK293T cells, but not untransfected HEK293T cells (Fig. S6A). In cells transfected with Piezo1 and TRPA1, an ion channel known to be expressed at the plasma membrane, we observed some overlap of Piezo1 staining with that of TRPA1 on the cell surface (24), although most Piezo1 and TRPA1 was present inside the cell (Fig. S6B). Thus Piezo1 protein can be localized at or near the plasma membrane. We could not detect expression of endogenous Piezo1 protein in N2A cells with this antibody.

Requirement of Piezo2 for rapidly-adapting MA currents in dorsal root ganglia neurons

To characterize Piezo2 expression within the heterogeneous population of neurons and glial cells of the DRGs, we performed *in situ* hybridization on adult mouse DRG sections (Fig. 6A). We observed Piezo2 mRNA expression in 20% of DRG neurons (from 2391 total neurons – see methods). Piezo2 was expressed in a subset of DRG neurons also expressing peripherin (60%) and Neurofilament 200 (28%), markers present in mechanosensory neurons (25-28) (Fig. S7). Some overlap with nociceptive marker TRPV1 (24%) further suggests a potential role of Piezo2 in noxious mechanosensation. We used siRNA transfection to examine the role of Piezo2 in MA currents of DRG neurons. RNAi on DRG neurons were validated on TRPA1, an ion channel expressed in DRG neurons and activated by mustard oil (MO) (29-30) (Fig. S8A-B). siRNAs against Piezo2 were validated in N2A cells overexpressing Piezo2 cDNA (Fig. S8C). We recorded whole-cell MA currents from DRG neurons transfected with GFP and either scrambled or Piezo2 siRNA ($n = 101$ for scrambled, and $n = 109$ for Piezo2 siRNA). We grouped the recorded MA currents according to their inactivation kinetics (Fig. 6B) (8-9,19-20,22). We defined four different classes of neurons based on τ_{inac} distribution in scrambled siRNA transfected cells (Fig. S8D): $\tau_{\text{inac}} < 10$ ms, $10 < \tau_{\text{inac}} < 30$, $\tau_{\text{inac}} > 30$ ms, and non-responsive neurons. The proportion of neurons expressing MA currents with $\tau_{\text{inac}} < 10$ ms was specifically and significantly reduced in neurons transfected with Piezo2 siRNA compared to that of neurons transfected with scrambled siRNA (Fig. 6C). 28.7% of scrambled siRNA-transfected neurons had $\tau_{\text{inac}} < 10$ ms compared to 7.3% in Piezo2 siRNA-transfected neurons (Fig. 6D). Neurons with MA currents with slower kinetics (τ_{inac} between 10 and 30 ms and $\tau_{\text{inac}} > 30$ ms) were present at normal proportions in cells transfected with Piezo2 siRNA. We observed a trend towards increased numbers of mechanically insensitive neurons in populations expressing Piezo2 siRNA, as predicted if loss of Piezo2 converts rapidly adapting neurons into non-responders. We also analyzed these RNAi data according to the

degree of current inactivation during the 150 ms test pulse and came to similar conclusions (Fig. S8E).

Discussion

We found that Piezo1 is required for MA currents in Neuro2A cells and Piezo2 is required for a subset of MA currents in DRG neurons. Moreover, overexpressing Piezo1 or Piezo2 in three different cell types gave rise to 17- to 300-fold increase in MA currents. We conclude that Piezos are both necessary and sufficient for the expression of a MA current in various cell types.

Piezo1 and Piezo2 sequences do not resemble those of other known ion channels or other protein classes. The large number of predicted transmembrane domains of Piezo1 and Piezo2 is reminiscent of the structure of voltage-activated sodium channels with 24 transmembrane domains, composed of a 4-fold repeat of 6-transmembrane units (31). However, pore-containing or repetitive domains have not been observed in Piezo proteins. It may be that Piezo proteins are non-conducting subunits of ion channels required for proper expression or for modulating channel properties, similar to beta subunits of voltage-gated channels (31) or SUR subunits of ATP-sensitive K⁺ channels (32). In this case, all the cell types used here would have to express an inactive conducting subunit of an MA channel that requires Piezos to function. Alternatively, Piezo proteins may define a distinct class of ion channels, akin to Orai1, which lacks significant sequence homology to other channels (33). Piezo1 is also found in the endoplasmic reticulum (14-15), so Piezos may act at both the plasma membrane and in intracellular compartments.

We described a role of Piezo2 in rapidly-adapting mechanically-activated currents in somatosensory neurons. Thus Piezo2 has potential roles in touch and pain sensation (34-35). Piezo 1 and 2 are expressed in various tissues, and their homologs are present throughout animals, plants, and protozoa, raising the possibility that Piezo proteins have a broad role in mechanotransduction.

Supplementary Material

Refer to Web version on PubMed Central for supplementary material.

Acknowledgments

The authors gratefully acknowledge H. Hu for help in cloning Piezo2, J. Walker for contributing to microarray experiments, S. Batalov for help in bioinformatics analysis, K. Spencer for help with imaging, N. Hong and U. Müller for comments on the manuscript and helpful discussions. Supported by grants from the NIH (DE016927, NS046303) and Novartis Research Foundation. B.C. is the recipient of an American Heart Association postdoctoral fellowship; M.S., German Academic Exchange Service (DAAD, D/07/41089) fellowship.

References

1. Chalfie M. *Nat Rev Mol Cell Biol.* Jan.2009 10:44. [PubMed: 19197331]
2. Hamill OP, Martinac B. *Physiol Rev.* Apr.2001 81:685. [PubMed: 11274342]
3. Monshausen GB, Gilroy S. *Trends Cell Biol.* May.2009 19:228. [PubMed: 19342240]
4. Iwatsuki K, Hirano T. *Comp Biochem Physiol A Physiol.* Feb.1995 110:167. [PubMed: 7704627]
5. Corey DP, Hudspeth AJ. *Biophys J.* Jun.1979 26:499. [PubMed: 318064]
6. McCarter GC, Reichling DB, Levine JD. *Neurosci Lett.* Oct 8.1999 273:179. [PubMed: 10515188]
7. Praetorius HA, Spring KR. *J Membr Biol.* Nov 1.2001 184:71. [PubMed: 11687880]
8. Coste B, Crest M, Delmas P. *J Gen Physiol.* Jan.2007 129:57. [PubMed: 17190903]
9. Drew LJ, Wood JN, Cesare P. *J Neurosci.* Jun 15.2002 22:RC228. [PubMed: 12045233]

10. Besch SR, Suchyna T, Sachs F. *Pflugers Arch.* Oct.2002 445:161. [PubMed: 12397401]
11. Cho H, et al. *Eur J Neurosci.* May.2006 23:2543. [PubMed: 16817857]
12. Earley S, Waldron BJ, Brayden JE. *Circ Res.* Oct 29.2004 95:922. [PubMed: 15472118]
13. Sharif-Naeini R, et al. *Cell.* Oct 30.2009 139:587. [PubMed: 19879844]
14. Satoh K, et al. *Brain Res. Sep 7.2006 1108:19.* [PubMed: 16854388]
15. McHugh BJ, et al. *J Cell Sci.* Jan 1.2010 123:51. [PubMed: 20016066]
16. Hynes RO. *Cell. Sep 20.2002 110:673.* [PubMed: 12297042]
17. Burnstock G. *Mol Pain.* 2009; 5:69. [PubMed: 19948030]
18. Rodat-Despoix L, Delmas P. *Pflugers Arch.* May.2009 458:179. [PubMed: 19153764]
19. Hu J, Lewin GR. *J Physiol.* Dec 15.2006 577:815. [PubMed: 17038434]
20. Drew LJ, et al. *J Physiol.* May 1.2004 556:691. [PubMed: 14990679]
21. Drew LJ, et al. *PLoS ONE.* 2007; 2:e515. [PubMed: 17565368]
22. Wetzell C, et al. *Nature.* Jan 11.2007 445:206. [PubMed: 17167420]
23. Hao, J., et al. *Mechanosensitivity of the Nervous System.* K., I.; Kamkin, A., editors. Vol. vol. 2. Springer; Netherlands: 2008. p. 51-67.
24. Schmidt M, Dubin AE, Petrus MJ, Earley TJ, Patapoutian A. *Neuron.* Nov 25.2009 64:498. [PubMed: 19945392]
25. Goldstein ME, House SB, Gainer H. *J Neurosci Res.* Sep.1991 30:92. [PubMed: 1795410]
26. Lawson SN. *Exp Physiol.* Mar.2002 87:239. [PubMed: 11856969]
27. Lawson SN, Harper AA, Harper EI, Garson JA, Anderton BH. *J Comp Neurol.* Sep 10.1984 228:263. [PubMed: 6434599]
28. Sann H, McCarthy PW, Jancso G, Pierau FK. *Cell Tissue Res.* Oct.1995 282:155. [PubMed: 8581918]
29. Bandell M, et al. *Neuron.* Mar 25.2004 41:849. [PubMed: 15046718]
30. Jordt SE, et al. *Nature.* Jan 15.2004 427:260. [PubMed: 14712238]
31. Hanlon MR, Wallace BA. *Biochemistry.* Mar 5.2002 41:2886. [PubMed: 11863426]
32. Tucker SJ, Ashcroft FM. *Curr Opin Neurobiol.* Jun.1998 8:316. [PubMed: 9687347]
33. Prakriya M, et al. *Nature.* Sep 14.2006 443:230. [PubMed: 16921383]
34. Basbaum AI, Bautista DM, Scherrer G, Julius D. *Cell.* Oct 16.2009 139:267. [PubMed: 19837031]
35. Lewin GR, Moshourab R. *J Neurobiol.* Oct.2004 61:30. [PubMed: 15362151]

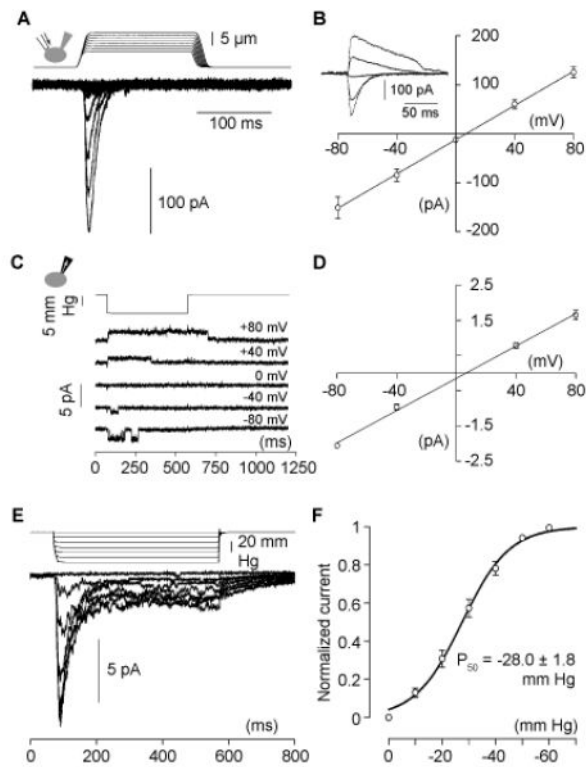


Fig. 1. Mechanically-activated currents in Neuro2A cells

(A) Representative traces of mechanically-activated (MA) inward currents expressed in Neuro2A (N2A) cells. Cells were subjected to a series of mechanical steps of $1\ \mu\text{m}$ movements of a stimulation pipette (inset drawing, arrow) in the whole-cell patch configuration at a holding potential of $-80\ \text{mV}$. (B) Average current-voltage relationships of MA currents in N2A ($n = 11$) cells. Inset, representative MA currents evoked at holding potentials ranging from -80 to $+40\ \text{mV}$ (applied $0.7\ \text{sec}$ prior to the mechanical step). (C) Single-channel currents (cell attached patch configuration) induced by negative pressure with a pipette (inset drawing, arrow) at holding potentials ranging from $-80\ \text{mV}$ to $+80\ \text{mV}$ in a N2A cell. (D) Average current-voltage relationships of stretch-activated single channels in N2A cells ($n = 4$, mean \pm SEM). Single channel conductance was calculated from the slope of the linear regression line of each cell giving $\gamma = 22.9 \pm 1.4\ \text{pS}$ (mean \pm SEM). Single channel amplitude was determined as the amplitude difference in Gaussian fits of full trace histograms. (E) Representative currents (averaged traces) induced by negative pipette pressure (0 to $-60\ \text{mm Hg}$, $\Delta 10\ \text{mm Hg}$) in a N2A cell. (F) Normalized current-pressure relationship of stretch activated currents at $-80\ \text{mV}$ fitted with a Boltzmann equation ($n = 21$). P_{50} is the average value of P_{50} s from individual cells.

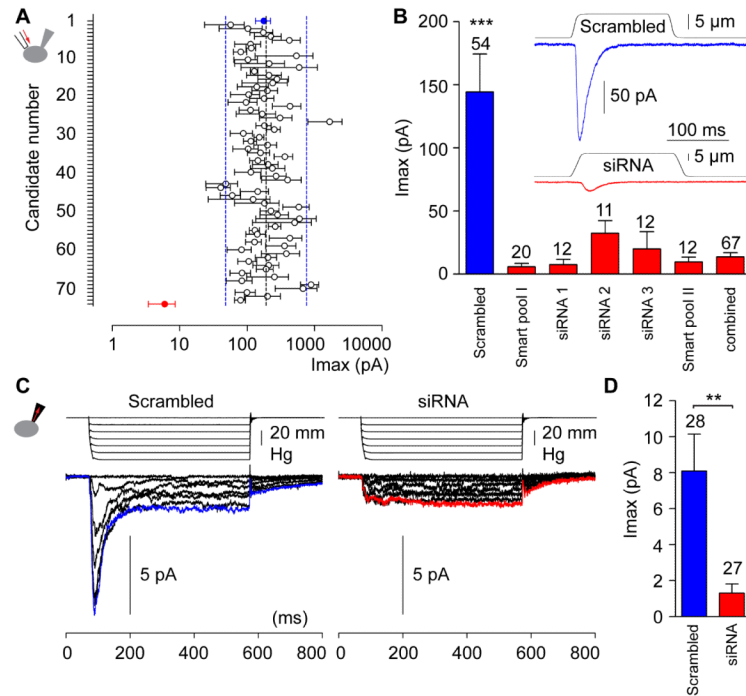


Fig. 2. Suppression of mechanically-activated currents by Piezo1 (Fam38A) siRNA

(A) Average maximal amplitude of MA inward currents elicited at a holding potential of -80 mV in N2A cells transfected with scrambled siRNA (blue dot, $n = 56$), Piezo1 (Fam38A) siRNA (red dot, $n = 20$) or siRNA directed against other candidates tested (open symbols, list of candidates available in Table S1). For each candidate, black circle and error bar represents the mean \pm SEM, $n = 4$ -27 each. The black line represents the average value of all cells tested ($n = 807$) and the two blue dashed lines represent 4-fold decrease or increase of this value. (B) Average maximal amplitude of MA inward currents elicited at a holding potential of -80 mV in N2A cells transfected either with scrambled siRNA (blue) or different Piezo1 (Fam38A) siRNAs (red). Smart-pool I is composed of four siRNAs including siRNA 1, 2 and 3. ***, $P < 0.001$, Kruskal-Wallis test. Inset: Representative traces of MA inward currents expressed in N2A cells transfected with scrambled siRNA (blue trace) or Piezo1 (Fam38A) siRNA (red trace) at a holding potential of -80 mV. (C) Representative currents (averaged traces) induced by negative pipette pressure (0 to -60 mm Hg, $\Delta 10$ mm Hg, cell attached) in a N2A cell transfected with scrambled siRNA (left panel) or Piezo1 siRNA (right panel). Traces of current elicited by -60 mm Hg are highlighted in blue and red. (D) Average maximal amplitude of stretch-activated currents elicited at a holding potential of -80 mV in N2A cells transfected with scrambled siRNA (blue) or Piezo1 siRNA (red). Bars represent the mean \pm SEM, and the number of cells tested is shown above the bars. **, $P < 0.01$, unpaired t-test with Welch's correction.

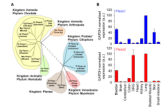


Fig. 3. Evolutionary conservation and expression profile of mouse *Piezo1* and *Piezo2*

(A) Unrooted phylogenetic tree showing sequence relationship of different members of the Piezo family of proteins. The alignments were generated using Megalign and DrawTree programs. The dotted line represents an artificially extended line to accommodate fit. Hs, Homo Sapiens; Mm, Mouse musculus; Gg, Gallus gallus, Dr, Danio Rerio; Ci, Ciona intestinalis; Dm, Drosophila melanogaster; Ce, Caenorhabditis elegans; Dd, Dictyostelium discoideum; At, Arabidopsis thaliana; Os, Oryza sativa; Tt, Tetrahymena thermophila (accession numbers are provided in Methods). Protista is referred to as a single kingdom, but can be considered as a group of diverse phyla (B) mRNA expression profiles of *Piezo1* (upper panel) and *Piezo2* (lower panel) determined by qPCR from various adult mouse tissues. GAPDH was used as the reference gene and lung as the tissue calibrator using the $2^{-\Delta\Delta CT}$ method. Each bar is the mean + SEM of the average of two separate experiments.

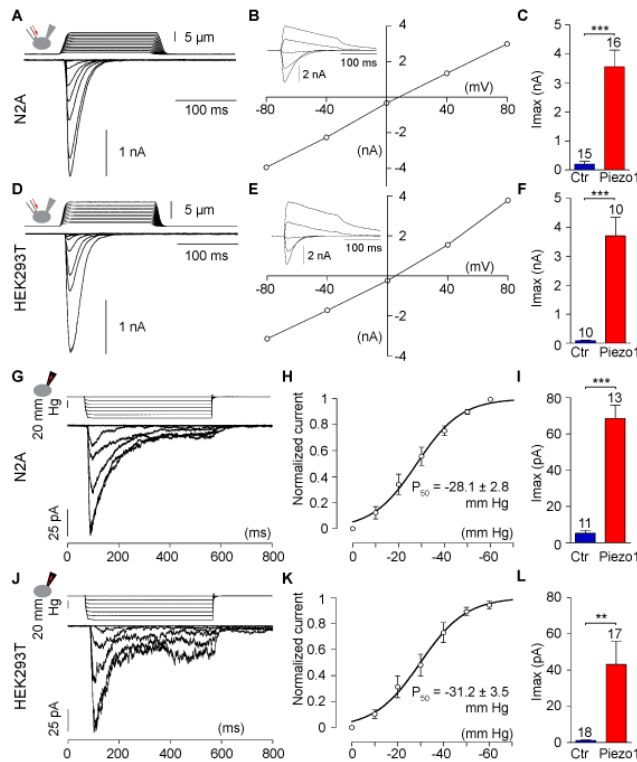


Fig. 4. Large mechanically-activated currents from cells overexpressing Piezo1
 (A-F) MA currents of Piezo1-expressing N2A (A-C) and HEK293T (D-F) cells recorded in the whole-cell configuration. (A, D) Representative traces of MA inward currents expressed in different cell types transfected with Piezo1. Cells were subjected to a series of mechanical steps in 1 μm (A) or 0.5 μm (D) increments using glass probe stimulation and at a holding potential of -80 mV. (B, E) Representative current-voltage relationships of MA currents expressed in different cell types transfected with Piezo1. Inset, MA currents evoked at holding potentials ranging from -80 to +40 mV. (C, F) Average maximal amplitude of MA inward currents elicited at a holding potential of -80 mV in Piezo1-transfected (red) or mock-transfected (blue) cells. Bars represent the mean ± SEM, and the number of cells tested is shown above the bars. ***, P < 0.001, unpaired t-test with Welch's correction. (G-L) Stretch-activated currents of mouse Piezo1-expressing N2A (G-I) and HEK293T (J-L) cells in cell-attached configuration. Representative averaged currents induced by negative pipette pressure (0 to -60 mm Hg, Δ 10 mm Hg) in a N2A (G) and HEK293T (J) cells transfected with Piezo1. Imax normalized current-pressure relationship of stretch-activated currents elicited at -80 mV in Piezo1-transfected N2A (H, n = 12) and HEK293T (K, n = 11) cells and fitted with a Boltzmann equation. P₅₀ is the average value of all P₅₀s determined for individual cells. Average maximal amplitude of stretch-activated currents elicited at a holding potential of -80 mV in N2A (I) and HEK293T (L) cells mock-transfected (blue) or transfected with Piezo1 (red). Bars represent the mean ± SEM, and the number of cells tested is shown above the bars. ***, P < 0.001. **, P < 0.01, unpaired t-test with Welch's correction.

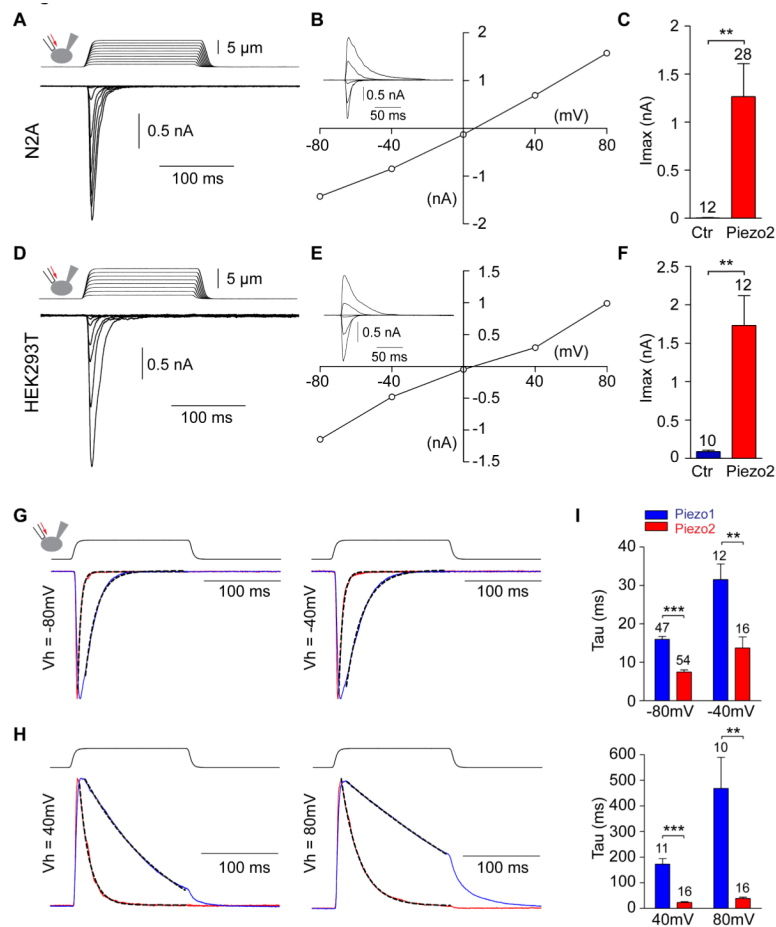


Fig. 5. Piezo2-dependent large mechanically-activated currents kinetically distinct from Piezo1-induced currents

(A-F) MA currents of Piezo2-expressing N2A (A-C) and HEK293T (D-F) cells in whole-cell configuration. In N2A cells, Piezo2 or vector only were transfected with Piezo1 siRNA to suppress endogenous Piezo1-dependent MA currents. (A, D) Representative traces of MA inward currents expressed in different cell types transfected with Piezo2. Cells were subjected to a series of mechanical steps of 1 μm movements of a glass probe at a holding potential of -80 mV. (B, E) Representative current-voltage relationships of MA currents expressed in different cell types transfected with Piezo2. Inset, MA currents evoked at holding potentials ranging from -80 to $+40$ mV. (C, F) Average maximal amplitude of MA inward currents elicited at a holding potential of -80 mV in Piezo1-transfected (red) or mock-transfected (blue) cells. (G-H) Representative traces of mechanically-activated inward (G) or outward (H) currents expressed in cells transfected with Piezo1 (blue trace) or Piezo2 (red trace) at the specified holding potentials. Traces were normalized to the peak current, and dashed lines represent fits of inactivation with a mono-exponential equation. (I) Time-constant of inactivation of Piezo1 (blue) and Piezo2 (red) at negative (-80 and -40 mV, upper panel) and positive (40 and 80 mV, lower panel) holding potentials. Bars represent the mean \pm SEM and the numbers above bars the number of cells. **, $P < 0.01$. ***, $P < 0.001$, unpaired t-test with Welch's correction.

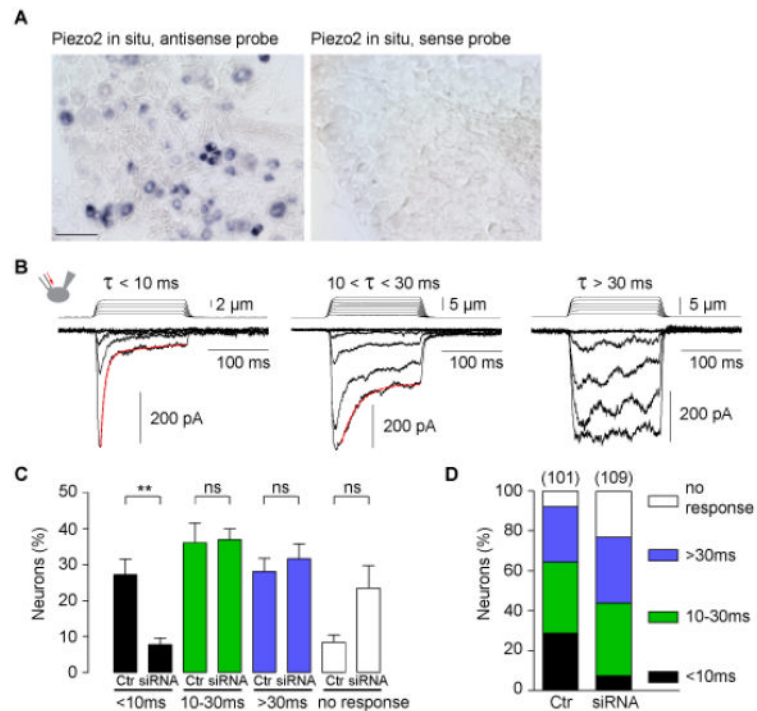


Fig. 6. Sensitivity of fast-inactivating MA currents in DRG neurons to depletion of Piezo2
 (A) Representative images of colorimetric in situ hybridization for Piezo2 in Dorsal Root Ganglia (DRG) neurons using antisense (left panel) and sense (right panel) probes. (B) Representative traces of three typical MA inward currents expressed in DRG neurons are characterized by distinct inactivation kinetics. Neurons were subjected to a series of mechanical steps in 1 μm increments at a holding potential of -80 mV. Current inactivation was fitted with a bi-exponential equation giving fast time-constant (τ) of 7.3 ms and slow time-constant > 100 ms (left panel), or with a mono-exponential equation giving a time constant of 27 ms (middle panel). Some currents with $\tau > 30$ ms are too slow to be efficiently fitted during the 150 ms lasting step stimulation (right panel). (C-D) Frequency histograms indicating the proportion of neurons transfected with scrambled siRNA (Ctr) or Piezo2 siRNA (siRNA) that respond to mechanical stimulation with MA currents characterized by their inactivation kinetic. Bars represent the mean \pm SEM of the proportion of neurons from seven separate experiments (B, $n = 12$ -19 neurons per condition and per experiment) or the proportion from all neurons pooled from all seven experiments (C); the numbers above bars in C represent the number of neurons. **, $P < 0.01$; ns, not significantly different; unpaired t test.